PHYSICAL REVIEW B VOLUME 47, NUMBER 8 15 FEBRUARY 1993-II

Si-adatom dynamics and mechanisms of the epitaxial growth on a single-height-stepped Si{001} surface

Deepak Srivastava and Barbara J. Garrison

Department of Chemistry, The Pennsylvania State University, University Park, Pennsylvania 16802

(Received 23 September 1992)

The Si-adatom dynamics on a single-height-stepped Si{001} surface is studied via a combined molecular-dynamics, simplified transition-state theory and time-dependent lattice-gas description using Tersoff's potential for Si-Si interactions. The energies of adatom binding and migration near S_A, $S_B(b)$ (bonded), and $S_B(n)$ (nonbonded) step edges show that the global minima, 4.28 eV, are in the trenches at the $S_B(n)$ edges. At all other sites, the binding energies are comparable to those on the flat Si{001}-(2×1) surface. We find that if the adatoms are deposited on an S_B terrace, reflection dominates at the S_A edge, whereas at the $S_B(b)$ and $S_B(n)$ edges, adatoms step down and migrate in the trenches parallel to the edges. The deposition rate and surface-temperature-dependent reflection, step up, step down, and accommodation probabilities at all three step edges are calculated and used in a simple estimation of step-edge growth coefficients. We find that the allowable surface-temperature range in which a 400-Å-wide S_B terrace may grow at the $S_B(b)$ and $S_B(n)$ edges is above 800 K for the 0.30 ML/min (where ML denotes monolayer) film deposition rate and above 700 K for the slower 0.03 ML/min film deposition rate. A microscopic model of the growth of S_B terraces is also presented in which we find that the nature of the growth, by accommodation, at the $S_B(b)$ and $S_B(n)$ edges, is different such that it maintains the roughness of the growing edge of an S_B terrace.

I. INTRODUCTION

In many experimental studies of layer-by-layer growth on the single-height-stepped Si{001} surface it has been observed that growth occurs predominantly at one of the step edges,[1,2] and that the dynamics near step edges can be used in controlling the shape and compositions of growing microstructures such as quantum wires and quantum grids.[3] This has caused an increased interest in understanding the step edges and their effect on surface processes during epitaxial growth dynamics.[1–7] In other experiments, epitaxially grown Ge/Si superlattices and alloys are shown to exhibit ordering which can be resolved to within 2–3-Å atomic separation.[8,9] The observed ordering in thin superlattices and alloys grown on Si{001} crystal faces is explainable only by models which require detailed dynamics of the deposited adatoms near single-height step edges on Ge and Si{001} surfaces.[10] From a theoretical perspective, even though many recent studies have focused on equilibrium structures,[5,7,11,12] surface elastic properties,[13,14] and temperature- and miscut angle-dependent phase diagrams[15,16] of the stepped Si{001} surface, the studies of the dynamics of the deposited adatoms near step edges are relatively absent. To our knowledge, only in very recent theoretical studies[17(a),17(b)] have attempts been made to identify Si adatom binding and migration near single-layer high steps on the Si{001} surface. Using the Stillinger-Weber potential for Si-Si interactions,[18] binding sites near S_A, $S_B(b)$ (bonded), and $S_B(n)$ (nonbonded) edges, their relative binding energies and migration barriers have been calculated.[17(a),17(b)] Following Chadi's nomenclature,[7] S_A-type steps and the S_A step edges have upper terrace dimer rows parallel to the step edge [Fig. 1(a)] and S_B-type steps and the $S_B(b)$ and $S_B(n)$ step edges [Figs. 2(a) and 3(a)] have upper terrace dimer rows perpendicular to the step edges. Even though binding energies and kinetics of migration near step edges have been reported,[17(a),17(b)] the long-range (covering from a few hundred to 1000 Å) and long time-scale (lasting up to a few milliseconds) dynamics of the adatom, as a function of surface temperature and film deposition rates, has not been attempted. We believe that this latter information is needed to make any realistic model of the epitaxial growth on stepped surfaces.

In this work we report the long time-scale and long-range dynamics of a Si adatom on a single-height-stepped Si{001} surface. Using Tersoff's potential for Si-Si interactions,[19] we have used a recently proposed combined molecular dynamics (MD), simplified transition-state theory (STST), and time-dependent lattice-gas (LG) method[20–22] to study the dynamics of an adatom as a function of experimentally significant film deposition rates and substrate temperatures. The combined MD-STST-LG approach exploits the strength of each technique in incorporating long time-scale and long-range dynamics on stepped surfaces in epitaxial growth studies. The role of MD is to study adsorption on clean terraces and map out adatom-surface interaction energy profiles for diffusive motions. The STST technique uses energies and forces on the computed energy profile to provide time constants and probabilities of diffusive jumps, which are then put together in a time-dependent LG simulation to study experimentally significant dynamics such as reflection, step up, step down, and accommodation near step edges. A quantitative knowledge of the dynamics at

 ©1993 The American Physical Society

step edges enables us to present a microscopic model of the growth of S_B terraces at step edges.

The energies of the adatom binding and migration near S_A, $S_B(b)$, and $S_B(n)$ step edges show that the global energetic minima are in the trenches at the $S_B(n)$ edges. This is in agreement with a similar study[17(a)] based on the Stillinger-Weber potential[18] for the atomic Si interactions. At the S_A and $S_B(b)$ edges the binding energies at all the sites are comparable to those on the flat Si{001} (2×1) (Ref. 21) surface using the same Si potential as in this work.[19] We find that the epitaxial growth dynamics near all three step edges is primarily decided by the long-time migration behavior. The results of LG "trajectories" for various film deposition rates and surface temperatures show that, if the adatoms are deposited on an S_B terrace, reflection is strong at the S_A edge whereas at the $S_B(b)$ and $S_B(n)$ edges adatoms step down and migrate in the trenches parallel to the step edges. The film deposition-rate- and surface-temperature-dependent reflection, step-up, step-down, and accommodation probabilities at all three step edges are calculated. These are used in a simple estimation of the surface-temperature- and deposition-rate-dependent growth coefficient—the fraction of the total deposited adatoms leading to the growth—of S_B terraces at step edges. On a 400-Å-wide S_B terrace the computed maximum growth coefficient at the $S_B(b)$ and $S_B(n)$ edges, 0.90 at 900 K, and a film deposition rate of 0.03 ML/min, is in good agreement with the experimental observations.[1,2] We propose a microscopic model of the epitaxial growth of the S_B terraces at the step edges in which the nature of the growth, by accommodation, at the $S_B(b)$ and $S_B(n)$ edges is

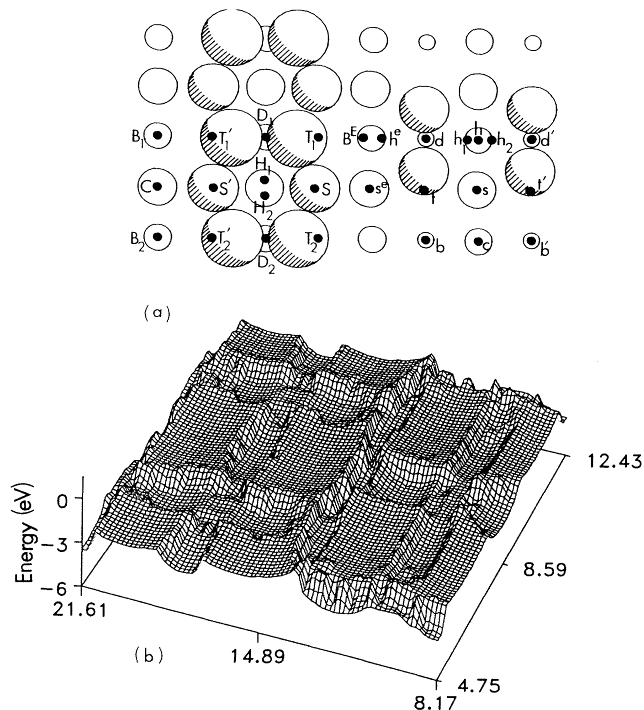

FIG. 1. The structure and energetics near an S_A edge on the Si{001} surface. (a) The surface unit cell with unique binding sites labeled. The sites on the upper terrace are labeled in upper case letters and those on the lower terrace in the lower case letters. The step-edge sites have additional superscripts e or E. (b) Energy profile for single adatom dynamics near the edge shown in (a).

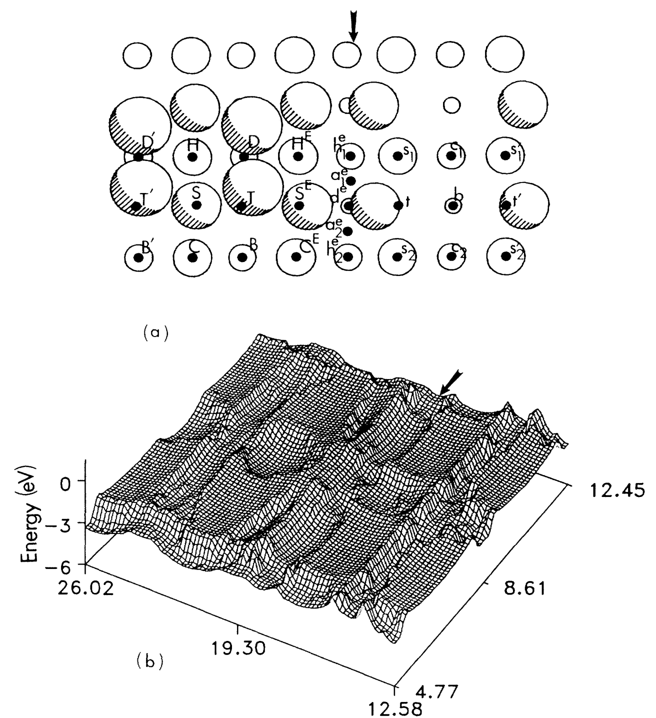

FIG. 2. Same as Fig. 1 for the dynamics near an $S_B(b)$ edge.

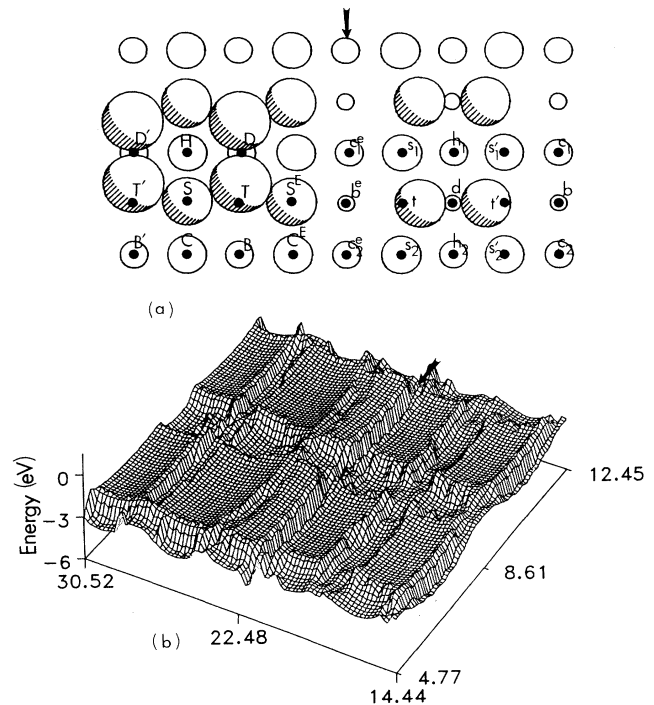

FIG. 3. Same as Fig. 1 for the dynamics near an $S_B(n)$ edge. Note that the global minima are at the b^e-type sites.

different such that the roughness of the growing edge of an S_B terrace is maintained.

In Sec. II, we briefly discuss the theoretical approach to the long time-scale and long-range dynamics on the stepped surfaces. Section III contains adatom-surface interaction energy profiles near S_A, $S_B(b)$, and $S_B(n)$ edges and a brief discussion of the energies of the binding and migration near step edges. In Sec. IV results of time-dependent LG simulations are presented including the calculated reflection, step up, step-down, and accommodation probabilities at all three step edges. Section V contains our suggested model for the growth of S_B terraces and finally in Sec. VI we briefly summarize the main results of this work.

II. THEORETICAL APPROACH TO THE ADATOM DYNAMICS ON STEPPED SURFACES

If the long-range effects of surface stresses and strains due to the formation and relaxation of steps[13,14] on the adatom motion are ignored, then the adatom dynamics on stepped surfaces can be broken into two constituent components, i.e., the dynamics on defect-free clean terraces and the dynamics near step edges. The Si and Ge adatom dynamics on clean terraces, being the same as that on the flat Si{001} (2×1) surface, has been studied previously.[21,22] In the present work, using the same Tersoff's potential for Si-Si interactions,[19] we study the energetics and dynamics of a Si adatom near step edges and combine these with our previous work on the flat Si{001} (2×1) surface[21] to study long time-scale and long-range dynamics of a Si adatom on the single-height-stepped Si{001} surface.

The diffusive jumps of the adatom near the step edges are computed through the STST approach in the same manner as was done for the clean terraces.[21,22] In the present method the adatom migration is composed of random uncorrelated jumps between neighboring binding sites. It is assumed that the time between successive jumps is much longer than the time taken to complete a jump. This approximation is reasonable because adatom-surface and -edge atom interactions are strongly attractive in nature (binding energies are 2–4 eV). Consequently the total escape rate from any binding site A is[20,21]

$$k_A^{\mathrm{STST}} = \sum_i \nu_{Ai} \exp\left[-\frac{E_{Ai}}{kT}\right], \tag{1}$$

where the sum over i runs over all possible high probability escape directions from site A, E_{Ai} is the 0-K activation energy for an escape in direction i, and ν_{Ai} is the vibrational frequency for the jump Ai as given by

$$\nu_{Ai} = \prod_{j=1}^{3} \nu_A^j \Big/ \prod_{k=1}^{2} \nu_i^k . \tag{2}$$

Here ν_A^j and ν_i^k are real vibrational frequencies when the adatom is at the local minimum A and at the saddle point in direction i, respectively. These quantities can be evaluated from the positive eigenvalues of the (3×3) force constant matrices. In Eq. (1), it is assumed that the adatom can escape only along discrete, high-probability, escape directions. If the probability of escape in all directions is more or less the same and can be represented by a continuous function then the summation in Eq. (1) must be replaced by an integral. The validity of this assumption for migration on clean terraces has been established,[21] where it was found that the adatom from any binding site could escape along only two orthogonal directions. Near step edges, as discussed below, the escape directions need not be in two orthogonal directions but still can be discerned along high-probability escape routes.

The activation energies E_{Ai} and the vibrational frequencies ν_{Ai} for use in Eqs. (1) and (2) were computed on the 0-K adatom-surface interaction energy profiles. The details of the energy profile calculations for the adatom diffusion on the flat Si{001} (2×1) surface are already reported in our previous work.[21,22] Now we discuss the calculations of the energy profiles near step edges. The S_A, $S_B(b)$, and $S_B(n)$ step edges were created on a properly dimerized surface.[23] The stepped structures were 10 layers deep. The bottom layer was held fixed and the remaining layers were allowed to relax through standard MD techniques.[24] All of the moving atoms were heated to 1000 K for 1–3 ps (Ref. 25) and then slowly cooled during which individual components of the velocity of each atom were independently set to zero as they passed through a maximum value.[21] As the kinetic energy of all the atoms was removed the total energy of the system was minimized. Periodic boundary conditions were used in both parallel and perpendicular directions to step edges to ensure that the surface and the bulk strains due to formation of steps were accommodated. The structures with S_A and $S_B(n)$ step edges had 11×4 atoms per layer and the structure with $S_B(b)$ step edge had 10×4 atoms per layer. We note that including more atoms in the system, by forming thicker and larger structures, does change the formation energies of the steps[11,12] but does not significantly affect the adatom-steps interaction energies[17(a)] which are the differences in the total energies of the system in the presence and the absence of the adatom. During relaxation in the presence of the adatom we kept the bottom five layers fixed to their fully relaxed configurations in the absence of the adatom, and allowed the top five layers to move according to Tersoff's potential.[26] To further reduce the number of moving atoms during the relaxations, in the presence of the adatom, we kept periodic boundary conditions only along the direction parallel to the step edges. In the other direction, i.e., perpendicular to the step edges, we fixed one column of atoms at the edges to simulate hard walls at the cell edges. The changes in the adatom-steps interaction energies due to these extra fixed atoms, away from step edges, were within 1% of the values reported here.

The incoming adatom was constrained in a fixed lateral position near the step edges. The adatom was aimed at the surface with velocity corresponding to the kinetic energy of 0.026 eV. The entire system, with the adatom constrained to move only normal to the surface plane, was allowed to relax for about 1.5 ps (1 ps $=10^{-12}$ s). The entire system was then cooled slowly for 3–5 ps as ex-

plained above. As the system was cooled to near 0 K the total energy of the system minimized and simultaneously the normal force on the adatom went to zero. The energy difference between the total energy of this system and that of the fully relaxed structure with no adatom was recorded as the adatom-step interaction energy. The procedure was repeated for a grid of lateral positions within an appropriate cell at the step edges. The initial grid spacing was 0.24 Å. For refinement of the minima and the saddle-point locations grid spacings as small as 0.04 Å were used. The convergence of the reported energies at all minima were checked with respect to the variations in MD times for the incoming adatom (1–3 ps) and the simulation temperature of the stepped structure (300–1000 K) atoms. The results reported here remain converged to within 1%. Of note is that the cooling procedure brings the system to 0 K, thus the only temperature dependence in the computed rates and probabilities of escape is through the Boltzmann factor in Eq. (1). In any real system the activation energies and vibration frequencies will also be modified by the thermal vibrations of step-edge atoms in the presence of the adatom. But given the uncertainties in the empirical potential the approximate first-order corrections[21] to the harmonic escape rates of Eq. (1) are not necessary.

We note that the vibration frequencies of jumps, ν_{Ai}, as needed in Eq. (1) are computed from real harmonic vibration frequencies at the minima and the saddle-point locations [Eq. (2)]. In our earlier work on a Si adatom diffusion on the flat Si{001} surface,[21] using the same Tersoff's potential[19] as used here, we found that the computed vibrational frequencies do not vary much within a single site and also from one site to another. The magnitude and anisotropy of migration is therefore largely determined by the activation energies of the migration jumps. We found that all the computed vibrational frequencies for the flat Si{001} surface are between 0.14×10^{13}/s and 0.95×10^{13}/s.[21] In this work we do not calculate vibrational frequencies from the positive eigenvalues of the force constant matrices. Instead we assume that near step edges the dynamics is determined mainly by migration barriers, and that the vibrational frequencies remain uniform with an average value of 0.4×10^{13}/s for all possible jumps. This assumption is reasonable because the initial goal is to examine the general nature of the dynamics near step edges and order of magnitude differences in reflection and accommodation processes at the step edges.

The next step in the calculation is to use the computed escape rates and jump probabilities in a time-dependent LG simulation to compute long time-scale and long-range dynamics on stepped surfaces. The time taken to escape from a site A is the inverse of the total escape rate k_A of Eq. (1) and the probability for accepting a jump in a direction i is equal to the ratio k_{Ai}/k_A. The adatoms are randomly deposited, weighted by the computed adsorption probabilities on the flat Si{001} (2×1) surface,[21] on an S_B-type terrace. The dynamics of the adatom proceeds by time increments determined from the total escape rates and the randomly selected directions of jumps weighted according to the computed jump probabilities. Each LG "trajectory" of the migrating adatom is run for long-time durations which are chosen, as will be shown below, according to the experimental deposition rates. During each run a record is kept of whether the adatom is reflected by a step edge, and how many times such reflections occur. The nature of the LG "trajectory" during the run and the final position of the adatom at the end of the "trajectory" determine if the adatom can be accommodated at a step edge or not.

III. BINDING ENERGIES AND MIGRATION BARRIERS NEAR STEP EDGES

The interaction energy profiles for the adatom binding and migration near S_A, $S_B(b)$, and $S_B(n)$ step edges are shown in Figs. 1–3, respectively. In each of these figures there are two kinds of binding sites. First, there are the binding sites on the upper and lower terraces close to step edges but not in the trenches at the step edges. Second, there are the binding sites in the trenches at the step edges which cannot be assigned to either of the upper and lower terraces. On the flat Si{001} (2×1) surface we found six unique binding sites within each surface unit cell.[21] The locations and energies of the binding sites near step edges are similar in nature and thus follow a similar naming pattern. The six unique sites are the long bridge $B(2,4,2)$, the dimer bridge $D(2,4,2)$, the cave $C(4,2,2)$, the hollow $H(4,2,1)$, the $T(1,2,4)$, and $S(2,1,2)$ sites. The numbers in parentheses indicate the number of nearest neighbors of the adatom in the surface, second, and third layers, respectively. The twofold B and D sites are generally above fourth-layer Si atoms, the fourfold C and H sites are generally over third-layer Si atoms, the T sites are on top of the bulk-terminated surface dimer atoms, and the S sites are over second-layer Si atoms. The sites near step edges are in upper case letters for the upper terrace sites and in lower case letters for the lower terrace sites. The edge sites have additional superscripts E or e, indicating that these sites cannot be assigned to either the upper or the lower terrace. In some cases we have found that the original unique site is split into two similar sites. In such cases all sites are identified distinctly. We finally note that as we move away from step edges similar sites within a cell are identified distinctly by superscript primes and double primes. In the following we describe the adatom binding and migration near step edges.

The binding energies of the sites near all three step edges in comparison with the similar sites on the flat Si{001} (2×1) surface[21] are listed in Table I. We note that the binding energies near step edges are not much different from those of the similar sites on the flat Si{001} surface. The maximum difference is about 10% in the binding at the H-type sites. For all other sites the difference is 6% or less. The binding energies of the sites in the trenches at the step edges are significantly different, therefore, we list these separately in Table II. The global minimum is at the b^e site in the trench at the $S_B(n)$ edge. The binding energy at a b^e site is 4.28 eV, and we note that the locations of this site are also in the epitaxial position if the growth were to nucleate at the

TABLE I. Binding energies near step edges.

Site	Binding energy[a] (eV)	Sites near step edges[b] (eV)	% difference
B	3.43	±0.19	6
D	3.26	±0.12	4
S	2.99	±0.14	5
H	2.57	±0.26	10
T	2.46	±0.05	2
C	2.37	±0.15	6

[a]Binding energies are for the sites on the flat Si{001} (2×1) surface (Ref. 21).
[b]Binding energies of sites near step edges in comparison with similar sites on the flat Si{001} (2×1) surface.

TABLE II. Binding energies in the trenches at the step edges.

S_A edges		$S_B(b)$ edges		$S_B(n)$ edges	
Site	Binding energy (eV)	Site	Binding energy (eV)	Site	Binding energy (eV)
B^E	3.07	H^E	1.96	c_1^e	3.73
h^e	3.19	S^E	2.89	S^E	2.53
s^e	2.84	C^E	2.65	b^{e} [a]	4.28
		h_1^e	2.76	C^E	3.04
		a_1^e	3.31	c_2^e	3.78
		d^e	3.43		
		a_2^e	3.25		
		h_2^e	2.95		

[a]The global minimum is at the b^e site at the $S_B(n)$ edge.

step edge. The b^e site is indeed the global minimum on the single-height-stepped Si{001} surface but the lifetime of the adatoms in this site, 0.3 μs (1 $\mu s=10^{-6}$ s) at 1000 K, is much less than the time in which the adatoms migrate, 0.01–10 ms (see below), during growth. Therefore, even though the b^e site has a higher probability of being the sink site on the single-height-stepped Si{001} surface, the overall growth behavior is decided by long-time migration near the step edges.

The migration barriers for the dynamics near an S_A edge are listed in Table III. As shown in Fig. 4 the adatoms are deposited on an S_B terrace. The adatoms approach the S_A edge from the lower terrace and the $S_B(b)$ and $S_B(n)$ edges from the upper terrace. We want to study reflection, step up or down and migration parallel to the step edges. At the S_A edge the migration jumps (Table III) important in facilitating these processes are $h \rightarrow h_1 \rightarrow d \rightarrow h^e$ type jumps on the lower terrace, $B^E \rightleftarrows s^e$ jumps in the trench parallel to the step edge, and $B^E \rightarrow T_1$ and $s^e \rightarrow S$ jumps for stepping up to the upper terrace, respectively (see Fig. 1). The migration in the trench, parallel to the S_A edge, is not feasible because the migration barriers for $s^e \rightarrow s^e$ (in the neighboring cell) jumps (1.48 eV) are much higher than those for the $s^e \rightarrow B^e$ jumps (0.14 eV). Therefore, instead of migrating parallel to the S_A edge the adatoms either preferably step-up on the upper terrace through $B^e \rightarrow T_1$ jumps or reflect back onto the S_B terrace. As shown in Fig. 4 the migrating adatoms generally approach the S_A edge via migration on top of the dimer rows and reflect back from the step edge via migration in the troughs between the dimer rows. We also note that the step-up at the S_A edge is basically a one-way process, i.e., the stepped-up adatoms cannot easily step down through $T_1 \rightarrow B^e$ or $S \rightarrow s^e$ jumps. This is because the adatoms step-up into D_1, H_1, H_2, and D_2 sites and migrate parallel to the S_A edge.

The migration barriers for the dynamics in the trenches at the $S_B(b)$ and $S_B(n)$ edges are listed in Tables IV and V, respectively. The deposited adatoms on an S_B terrace approach the $S_B(b)$ edge via $D' \rightleftarrows H \rightleftarrows D$ jumps (Fig. 2). The activation barrier to step-down through a $D \rightarrow H^e$ jump (2.05 eV) is twice as high as that for the reflection $D \rightarrow H$ jump (1.03 eV). To step down the adatoms instead make side excursions to S and T sites and then to C and B sites. The adatoms step-down in the trench through $T \rightarrow S^E$ and $B \rightarrow C^E$ jumps. The migration in the trench parallel to the step edge is through the sequence of jumps $h_1^e \rightleftarrows a_1^e \rightleftarrows d^e \rightleftarrows a_2^e \rightleftarrows h_2^e$. The maximum

TABLE III. Migration barriers near S_A edges.

Upper terrace to the trench		Dynamics in the trench		Lower terrace to the trench	
Jump type	Migration barrier (eV)	Jump type	Migration barrier (eV)	Jump type	Migration barrier (eV)
$T_1 \rightarrow B^E$	0.84	$B^E \rightarrow h^e$	0.96	$d \rightarrow h_1$	0.73
$T_1 \rightarrow S$	0.39	$B^E \rightarrow s^e$	0.37	$d \rightarrow t$	1.25
$T_1 \rightarrow D_1$	0.32	$B^E \rightarrow T_1$	1.44	$d \rightarrow h^e$	0.91
$S \rightarrow s^e$	1.79	$h^e \rightarrow d$	0.84	$t \rightarrow s$	0.35
$S \rightarrow T_1$	0.98	$h^e \rightarrow B^E$	1.09	$t \rightarrow d$	0.42
$S \rightarrow H_1$	0.70			$t \rightarrow s^e$	0.35
$S \rightarrow T_2$	1.05	$s^e \rightarrow t$	0.76	$t \rightarrow b$	0.52
		$s^e \rightarrow B^E$	0.14		
$T_2 \rightarrow b$	1.40	$s^e \rightarrow s^e(n)$	1.48	$b \rightarrow c$	1.02
$T_2 \rightarrow S$	0.47	$s^e \rightarrow S$	1.52	$b \rightarrow t$	1.45
$T_2 \rightarrow D_2$	0.41			$b \rightarrow T_2$	2.29

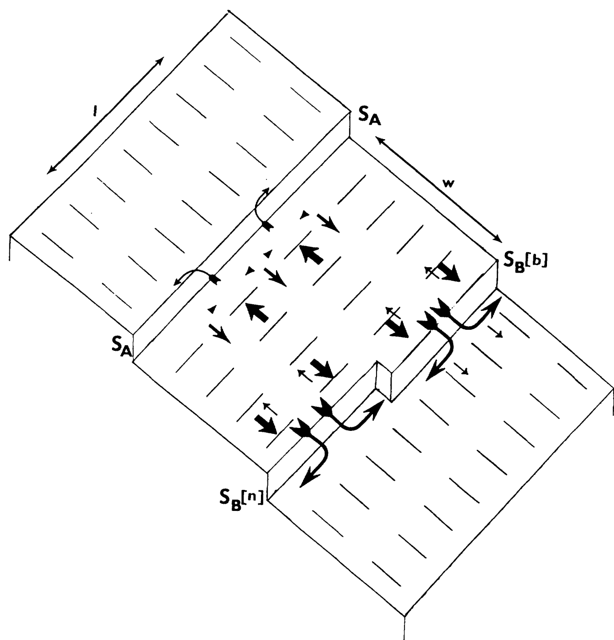

FIG. 4. A qualitative description of the adatom dynamics on an S_B terrace. The thick straight arrows are for the adatoms incident on the S_A, $S_B(b)$, or $S_B(n)$ edges. The curved arrows are for stepping up or down at the edges. The reflection is shown by thin straight arrows and the arrowheads near the S_A edge indicate that adatoms hover near the S_A edge but do not migrate parallel to the edge. At the $S_B(b)$ and $S_B(n)$ edges adatoms step down and migrate parallel to the edge (see text).

barrier to the parallel migration in the trench, 0.64 eV for an $a_1^e \rightarrow h_1^e$ jump, is less than the activation barrier for the overall diffusion on the flat Si{001} (2×1) surface (0.72 eV).[21] Therefore, the parallel migration in the trench is facile near the $S_B(b)$ edge. However, as opposed to the dynamics near the S_A edge, in this case the migrating adatoms can step-down in the trench, migrate parallel to the edge and escape out on to the upper S_B terrace or to the lower S_A terrace. In the dynamics near an $S_B(n)$ edge the migrating adatoms approach the edge from the upper terrace via $D' \rightarrow H$ and $H \rightarrow D$ jumps (Fig. 3). However, like near $S_B(b)$ edges, the adatoms do not directly step down via $D \rightarrow c_1^e$ jumps. The adatoms instead make side excursions to S, T and C, B sites and step down via $T \rightarrow S^E$ and $B \rightarrow C^E$ jumps, respectively. The migration barriers for all reverse step-up jumps from c_1^e, b^e, and c_2^e sites are fairly high. Therefore, once the adatoms step down in the trench at the $S_B(n)$ edge the adatoms stay in the trench and migrate parallel to the edge. We note that the maximum barrier to the parallel migration in the trench, 1.28 eV for a $b^e \rightarrow c_2^e$ jump, is about twice as high as that for the parallel migration in the trench at the $S_B(b)$ edge (0.64 eV). The parallel migration in the trench at the $S_B(n)$ edge, therefore, is much slower than the parallel migration in the trench at the $S_B(b)$ edge. Nevertheless, it can occur during the time scales of the typical epitaxial growth dynamics.

IV. LG SIMULATIONS: REFLECTION, STEP-UP, STEP-DOWN, AND ACCOMMODATION AT STEP EDGES

A knowledge of the overall dynamical behavior of the deposited adatoms on a stepped surface as a function of film deposition rate and surface temperature requires examining the long-range and long time-scale dynamics of the adatoms for various values of these parameters. A theoretical definition of the film deposition rates, however, needs to be established so that a comparison can be made with the experimental deposition rates. We construct a definition of the film deposition rates with the following approximations. The adatoms are deposited sequentially and each adatom can freely migrate on the surface until the next adatom is deposited. The lifetime of the migrating adatoms, equal to the time elapsed between two successive depositions, is assumed to be independent of the presence of the other adatoms and any other surface defects. The lifetime of the migrating adatoms together with the exposed surface area of an S_B-type terrace can define theoretical deposition rates in ML/min (ML stands for monolayer). In this work, for example, we sequentially deposit adatoms on a 1000×100 dimers^2 area of an S_B terrace (Fig. 4 with $l = 1000$ dimers and $w = 100$ dimers). An ideal monolayer of the deposited material on this surface contains 2×10^5 adatoms. If the adatoms are deposited at the rate of 1 adatom/ms (1 ms$=10^{-3}$ s) the overall deposition rate, under sequential deposition approximation, is 0.30 ML/min. We note that this is an approximate definition under ideal conditions. In experiments, adatom-adatom and adatom-surface defect interactions may not only change single adatom migration rates but the mean lifetime of each adatom may be much less than that considered in this definition. Our definition of the approximate deposition rates, therefore, is a lower bound on the comparable experimental deposition rates. We also note that because of the periodic boundary condition along the direction parallel to the step edges, we are simulating the LG dynamics on an infinite terrace length, l, parallel to the step edges. In contrast, the selected width, w, of 100 dimers (about 400 Å) perpendicular to the step edges is in accordance with the experimentally observed values of the equilibrium terrace widths.[1,2]

At this juncture, it is important to emphasize that the growth at step edges is possible only on the S_B terraces because the adatom migration on clean terraces is highly anisotropic in nature,[21,22,27–30] and only on the S_B terraces is the direction of fast migration perpendicular to the step edges. This implies that only on the S_B terraces will a sufficient number of the deposited adatoms reach step edges. On the S_A terraces, on the other hand, the direction of fast migration is parallel to the step edges. The migrating adatoms have a higher probability of finding each other and nucleating single dimer strings.[31–33] The nucleation and growth of such strings and their subsequent coalescence into the formation of anisotropic islands has been experimentally observed in scanning tunneling microscopic (STM) studies of the epitaxial growth on the Si{001} surface.[31–33]

The simulation of lattice-gas "trajectories" for each deposited adatom was performed at six temperatures between 600 and 1000 K. At each temperature we ran 1000 time-dependent random-walk "trajectories" weighted by the calculated jump probabilities for run times varying between 0.01 and 10.0 ms. The shortest run time of 0.01 ms corresponds to a deposition rate of 30 ML/min and the longest run time of 10.0 ms to a deposition rate of 0.03 ML/min. During each "trajectory," we recorded whether the adatom reached a step edge, stepped up or down, or reflected from the edge. In addition, other details of the dynamics near the step edge were monitored. During each "trajectory" an adatom can reach a step edge, reflect, and depending upon the S_B terrace width (100 dimers wide in our case) reach the other step edge. By the time a "trajectory" is completed the adatom, therefore, can be reflected many times from both the edges. On the other hand, in some "trajectories" the adatoms may not reach any of the step edges during the run and remain on the terrace on which they were originally deposited.

An analysis of the "trajectories" either not hitting a step edge or going through multiple hits at both the step edges is shown in Figs. 5(a) and 5(b), respectively. Any "trajectory" hitting both the edges at least once is counted as a multiple hit "trajectory." In Fig. 5(a) we note that at low temperatures (600–700 K) and fast deposition rates (30 and 3 ML/min) more than 84% of the "trajectories" do not reach any of the step edges. At higher temperatures (800–1000 K) and slower deposition rates (0.3 and 0.03 ML/min) more than 70% of the "trajectories" hit at least one of the edges. In fact at 900 and 1000 K almost all the "trajectories" hit one or the other edge. At these temperatures and film deposition rates [Fig. 5(b)] we note that more than 35% of the "trajectories" go through multiple hits at both the edges. The probability of no hit, a single hit, or multiple hits in a "trajectory" is mostly determined by the adatom migration rates on the flat Si{001} surface and the width of the S_B terrace on which the "trajectory" is propagated. Significant no hits at low temperatures and fast deposition rates mean that either the diffusion rates are too low or the terrace is too wide (100 dimers wide) to sustain the growth at the step edges. We note that our computed diffusion rates on the flat Si{001} (2×1) surface[21] [$D_{Si}=7.2\times10^{-4}\exp(-0.72\text{ eV/kT})\text{ cm}^2/\text{s}$] are in good agreement with the experimentally observed values.[30] On the basis of these "trajectories," therefore, we predict

TABLE IV. Migration barriers near $S_B(b)$ edges.

Upper terrace to the trench		Dynamics in the trench		Lower terrace to the trench	
Jump type	Migration barrier (eV)	Jump type	Migration barrier (eV)	Jump type	Migration barrier (eV)
$D\rightarrow H^E$	2.05	$H^E\rightarrow h_1^e$	0.02	$s_1\rightarrow c_1$	1.61
$D\rightarrow T$	1.22	$H^E\rightarrow S^E$	0.31	$s_1\rightarrow t$	1.05
$D\rightarrow H$	1.03	$H^E\rightarrow D$	0.08	$s_1\rightarrow h_1^e$	0.61
$T\rightarrow S^E$	0.42	$S^E\rightarrow d^e$	0.90	$t\rightarrow b$	0.58
$T\rightarrow D$	0.45	$S^E\rightarrow H^E$	1.24	$t\rightarrow s_1$	0.44
$T\rightarrow S$	0.52	$S^E\rightarrow T$	0.87	$t\rightarrow d^e$	0.21
$T\rightarrow B$	0.46	$S^E\rightarrow C^E$	0.63	$t\rightarrow s_2$	0.53
$B\rightarrow C^E$	0.85	$C^E\rightarrow h_2^e$	0.11	$s_2\rightarrow c_2$	1.77
$B\rightarrow T$	1.43	$C^E\rightarrow S^E$	0.39	$s_2\rightarrow t$	1.16
$B\rightarrow C$	0.99	$C^E\rightarrow B$	0.09	$s_2\rightarrow h_2^e$	0.52
		$h_1^e\rightarrow s_1$	0.34		
		$h_1^e\rightarrow a_1^e$	0.09		
		$h_1^e\rightarrow H^E$	0.82		
		$a_1^e\rightarrow h_1^e$	0.64		
		$a_1^e\rightarrow d^e$	0.46		
		$d^e\rightarrow t$	1.22		
		$d^e\rightarrow a_1^e$	0.58		
		$d^e\rightarrow S^E$	1.44		
		$d^e\rightarrow a_2^e$	0.62		
		$a_2^e\rightarrow d^e$	0.44		
		$a_2^e\rightarrow h_2^e$	0.44		
		$h_2^e\rightarrow s_2$	0.42		
		$h_2^e\rightarrow a_2^e$	0.14		
		$h_2^e\rightarrow C^E$	0.41		

TABLE V. Migration barriers near $S_B(n)$ edges.

Upper terrace to the trench		Dynamics in the trench		Lower terrace to the trench	
Jump type	Migration barrier (eV)	Jump type	Migration barrier (eV)	Jump type	Migration barrier (eV)
$D\rightarrow c_1^e$	2.17	$c_1^e\rightarrow s_1$	2.41	$s_1\rightarrow h_1$	0.73
$D\rightarrow T$	1.27	$c_1^e\rightarrow b^e$	0.70	$s_1\rightarrow t$	1.01
$D\rightarrow H$	1.46	$c_1^e\rightarrow D$	2.52	$s_1\rightarrow c_1^e$	1.77
		$c_1^e\rightarrow S^E$	2.13		
$T\rightarrow S^E$	0.68	$S^E\rightarrow b^e$	0.63	$t\rightarrow d$	0.34
$T\rightarrow D$	0.40	$S^E\rightarrow c_1^e$	0.93	$t\rightarrow s_1$	0.40
$T\rightarrow S$	0.52	$S^E\rightarrow T$	0.70	$t\rightarrow b^e$	0.17
$T\rightarrow B$	0.46	$S^E\rightarrow C^E$	0.71	$t\rightarrow s_2$	0.43
$B\rightarrow C^E$	1.03	$b^e\rightarrow t$	1.97	$s_2\rightarrow h_2$	0.57
$B\rightarrow T$	1.50	$b^e\rightarrow c_1^e$	1.25	$s_2\rightarrow t$	1.02
$B\rightarrow C$	1.21	$b^e\rightarrow S^E$	2.38	$s_2\rightarrow c_2^e$	1.76
		$b^e\rightarrow c_2^e$	1.28		
		$C^E\rightarrow c_2^e$	0.16		
		$C^E\rightarrow S^E$	1.22		
		$C^E\rightarrow B$	0.52		
		$c_2^e\rightarrow s_2$	2.47		
		$c_2^e\rightarrow b^e$	0.78		
		$c_2^e\rightarrow C^E$	0.90		

that on a 400-Å-wide S_B terrace at 600 K or lower temperatures and 3 ML/min or faster deposition rates the growth at the step edges[1,2] will not dominate over the nucleation and coalescence of anisotropic islands.[30–33] In the following, we will address the dynamics near S_A, $S_B(b)$, and $S_B(n)$ edges and compute reflection, step-up, step-down, and accommodation probabilities.

In computing the probabilities of dynamical events near step edges, we note that the analysis is done only for "trajectories" which hit either of the step edges at least once. At experimentally comparable deposition rates (0.30 and 0.03 ML/min), many "trajectories" undergo multiple hits at both edges. The probabilities at any edge, therefore, are computed from the total hits at only the same edge. A qualitative view of three types of dynamical events, i.e., reflection, hovering near the edge, and stepping up or down, is already shown in Fig. 4. At the S_A edge, we note that the reflection is strong but there is significant hovering near the edge. In the simulations we find that at higher temperatures the majority of the hovering adatoms either reflect or step up on the upper S_A terrace. At the $S_B(b)$ and $S_B(n)$ edges the hovering near the edges and the reflection are fairly weak and most of the adatoms step down in the trench and migrate parallel to the edge.

The quantitative behavior of the reflection, hovering, and step-up or step-down probabilities at all three step edges are shown in Figs. 6(a)–6(f). At the 0.03-ML/min deposition rate, the reflection probability at the S_A edge [Fig. 6(b)] peaks at a value of 0.88 at 800 K. The fall off in the values of the reflection probability at higher temperatures is because the step-up probability starts to increase significantly. At the 0.30-ML/min deposition rate

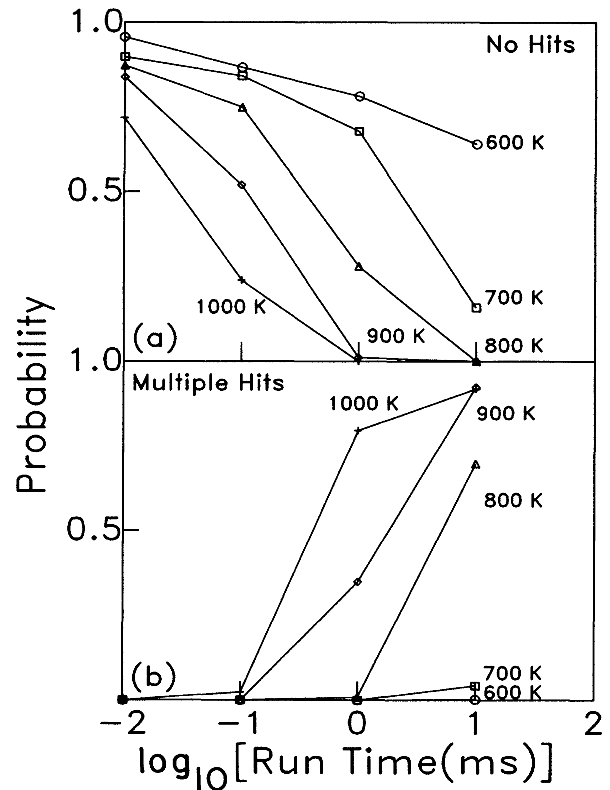

FIG. 5. The run time analysis on the S_B terrace of Fig. 4. (a) The probabilities of single adatom "trajectories" not hitting any edge. (b) The probabilities of single adatom "trajectories" undergoing multiple hits at both the edges (see text).

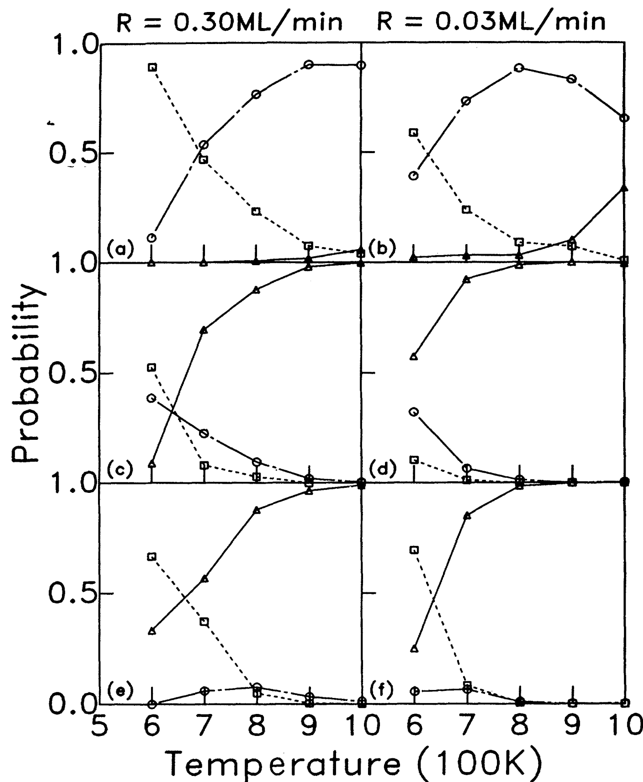

FIG. 6. The probabilities of three types of dynamical events near (a),(b) S_A, (c),(d) $S_B(b)$, and (e),(f) $S_B(n)$ edges. The circles with dash-dotted lines are for reflection at the edge, and the triangles with solid lines are the probabilities for stepping up or down at the edge. The squares with dashed lines are the adatoms hovering near the edge. Note that in (c) and (d) the step-down probabilities are for adatoms stepping down at least once in the trench at the $S_B(b)$ edge. For the fate of these adatoms see text and Table VI.

[Fig. 6(a)] the peaking behavior is not that significant because the step-up probability remains less than 0.05 at all temperatures. In contrast, at the $S_B(b)$ and $S_B(n)$ edges we note that at the higher temperatures (800–1000 K) for both deposition rates [Figs. 6(c)–6(f)] most of the adatoms step down in the trenches at the edges and migrate parallel to the edges. As noted earlier the adatoms in the trench at the $S_B(b)$ edge, however, can escape from parallel migrations and be counted as the "reflected" or "escaped to the lower terrace" adatoms. From Table VI, we note that more than 80% of the adatoms for both deposition rates at 800–1000 K do not remain in the trench at the end of the simulation. The fate of the adatoms which thus escaped from the trench at the $S_B(b)$ edge are listed as "reflection," "hovering," and "lost to the lower terrace" probabilities in Table VI. In Table VI, we also list the mean lifetimes that these adatoms spend in the trench. The mean lifetimes spent in the trench, for both deposition rates and at all temperatures, are greater than 0.03 ms. On the other hand, for a parallel migration in the trench even at 600 K, the maximum time constant for the escape, 1.3×10^{-8} s, is from a d^e site. Therefore, even at 600 K, the parallel migrating adatoms take at least roughly 10^3 jumps in the trench before escaping in either directions to the upper S_B or the lower S_A terraces. Consequently, in the final analysis, we can consider these adatoms to have enough time to migrate in the trench to find each other or the existing kink sites. This means that the probability of the accommodation at the $S_B(b)$ edge can be considered to be same as that of stepping down at least once in the trench at the $S_B(b)$ edge [Figs. 6(c) and 6(d)]. At the $S_B(n)$ edge the stepped down adatoms cannot escape from the trench. Therefore, the fate of such adatoms is to directly contribute towards accommodation at the $S_B(n)$ edge [Figs. 6(e) and 6(f)].

V. PROPOSED MECHANISM OF THE GROWTH OF S_B TERRACES

The combined MD-STST-LG method with Tersoff's potential for Si-Si interactions gives insights into microscopic mechanisms of growth of S_B terraces on a single-height-stepped Si{001} surface. We find that on a 400-Å-wide S_B terrace most of the deposited adatoms at 800–1000 K and for film deposition rates of 0.30–0.03 ML/min reach one of the edges. In this range of surface temperatures and film deposition rates, the reflection

TABLE VI. Fate of the adatoms that stepped down in the trench at the $S_B(b)$ edge.

Temperature (K)	Trench	Edge	Reflected	Escaped to lower terrace	Mean time in the trench (ms)
		Deposition rate 0.30 ML/min			
600	0.778	0.222	0.000	0.000	0.000
700	0.285	0.411	0.304	0.000	0.054
800	0.214	0.257	0.529	0.000	0.032
900	0.109	0.156	0.679	0.056	0.030
1000	0.078	0.078	0.675	0.169	0.041
		Deposition rate 0.03 ML/min			
600	0.429	0.381	0.190	0.000	0.42
700	0.246	0.251	0.498	0.005	0.35
800	0.106	0.136	0.714	0.044	0.20
900	0.108	0.058	0.618	0.216	0.14
1000	0.088	0.017	0.507	0.388	0.07

probability is more than 0.75 at the S_A edge. At the $S_B(b)$ or $S_B(n)$ edges adatoms preferably step down in the trenches and migrate parallel to the edges [Figs. 4 and 6(c)–6(f)]. The parallel migration of the adatoms in the trench at the $S_B(b)$ edges is more facile (maximum activation barrier is 0.64 eV) than in the trench at the $S_B(n)$ edges (maximum activation barrier is 1.28 eV). Therefore at the $S_B(b)$ edges the parallel migrating adatoms are more likely to find the existing kink sites, whereas at the $S_B(n)$ edges the adatoms may stay in the vicinity of where they initially hit the edge and nucleate new single dimer kinks with the other parallel migrating adatoms in the vicinity. At the $S_B(b)$ edges the accommodation at the existing kink sites will tend to smoothen the roughness of the edge, but at the $S_B(n)$ edges the random nucleation of new single dimer kinks will contribute towards the roughness of the edge. In the growth of the S_B terraces at the $S_B(b)$ and $S_B(n)$ edges, since both the edges occur alternately, the growth at the edges will be equally distributed between the random nucleation of new single dimer kinks and the accommodation at the existing kink sites. We believe, therefore, that the roughness of the edges of the growing S_B terraces will remain during the growth. Recent experimental observations of the growth of S_B terraces using STM indeed confirm this behavior of the edges during the growth.[1,2]

Combining the overall kinetics with the detailed probabilities at the S_A, $S_B(b)$, and $S_B(n)$ edges [Figs. 6(a)–6(f)] we can estimate the fraction of the deposited adatoms that will be accommodated at the $S_B(b)$ or the $S_B(n)$ edges of the 400-Å-wide terrace and the fraction that remain on the terrace contributing to the growth by nucleation and coalescence of anisotropic islands. The estimation of the accommodation coefficient at the $S_B(n)$ edges is straightforward because nearly all of the adatoms which step down in the trench remain at the edge. At the $S_B(b)$ edges, however, we have shown that all the adatoms which stepped down at least once in the trench spent enough time in the trench so as to directly contribute towards the growth at the edge. The full accommodation coefficient at an $S_B(b)$ edge of the growing terrace is computed by accounting for the losses to the neighboring S_A and S_B terraces, the adatoms hovering near the S_A and $S_B(b)$ edges, and the adatoms reflected from the S_A or $S_B(b)$ edges but have not yet reached the $S_B(b)$ or S_A edges, respectively. The probabilities of a deposited adatom either accommodating at the $S_B(b)$ edge or remaining on the S_B terrace are listed in Table VII. If we assume that all single adatoms which remain on the S_B terrace contribute towards the growth via nucleation and coalescence of anisotropic islands, we can relate the computed probabilities in Table VII to the coefficient of the growth of S_B terraces either at the edge or via nucleation and growth of anisotropic islands on the terrace. At a film deposition rate of 0.30 ML/min the growth coefficient of a 400-Å-wide S_B terrace at the $S_B(b)$ edge is only 0.01 at 600 K but increases to 0.85 at 1000 K. At the 0.03-ML/min deposition rate, however, we note that instead of increasing uniformly with temperature the edge growth coefficient peaks to about 0.88 at 900 K.

TABLE VII. Growth coefficients on an S_B terrace.

Temperature (K)	Islanding on the terrace	Growth at the edge
	Deposition rate 0.30 ML/min	
600	0.834	0.010
700	0.801	0.111
800	0.588	0.318
900	0.314	0.631
1000	0.092	0.854
	Deposition rate 0.03 ML/min	
600	0.768	0.103
700	0.479	0.398
800	0.135	0.789
900	0.032	0.878
1000	0.026	0.785

The fall in the edge growth coefficient at 1000 K as explained before is due to the higher step-up probability at the S_A edge. A similar behavior of the edge growth coefficient is also observed for the growth at the $S_B(n)$ edges. The allowable range of surface temperatures in which a 400-Å S_B terrace may grow at the $S_B(b)$ and $S_B(n)$ edge is above 800 K for the 0.30-ML/min film deposition rate and above 700 K for the slower 0.03-ML/min film deposition rate. It is clear from Table VII that below these critical temperatures most of the deposited adatoms on the S_B terrace will remain on the terrace and may contribute towards the growth via nucleation and coalescence of anisotropic islands. These estimates based on only a single adatom dynamics on a constant width S_B terrace are in qualitative agreement with recent experimental observations.[1,2] A quantitative comparison between theory and experimental growth observations can be made only if similar LG simulations are performed on S_B terraces of varying widths and adatom-adatom and adatom-surface defect interactions are also included in the dynamics.

VI. COMMENTS

The long-range and long time-scale dynamics of a Si adatom on the single-height-stepped Si{001} surface has been explored via a recently proposed MD-STST-LG method[20–22] using Tersoff's potential for Si interactions.[19] The binding energies near S_A, $S_B(b)$, and $S_B(n)$ edges show the global energetic minima 4.28 eV to be in the trenches at the $S_B(n)$ edges. The migration barriers for all possible jumps near all three steps are obtained. A brief examination of these migration barriers show possible parallel migration to the $S_B(b)$ and $S_B(n)$ edges in the trenches at the edges. These general characteristics of the adatom-step interaction energy profiles (Figs. 2 and 3) are in agreement with recent studies[17(a),17(b)] of the energetics of the same system using the Stillinger-Weber Si potential.[18] Near the S_A edge we find that the incident adatoms either step-up on the upper terrace or reflect from the edge. The adatoms, though, can be trapped near the edge but they do not migrate parallel to the

edge. In Ref. 17(b) it is noted that single adatoms neither step-up on the upper terrace and nor reflect from the edge. The adatoms are trapped near the edge and migrate parallel to the edge. We note that these differences are due to different potentials used in our work and in Ref. 17(b). Our observation of single adatom step-up and reflection dynamics near the S_A edge, however, are in better agreement with the experimental observations in which no nucleation or growth near the S_A edge is noted.[1,2]

In addition, in this work, we have calculated the surface temperature and the film deposition-rate-dependent reflection, hovering near the edge, and step-up and step-down probabilities at all three step edges. These are used in a model of the epitaxial growth of S_B terraces at the $S_B(b)$ and $S_B(n)$ edges. We find that the allowable surface temperature range in which a 400-Å-wide S_B terrace may grow at the $S_B(b)$ and $S_B(n)$ edges is above 800 K for the 0.30-ML/min film deposition rate and between 700 and 1000 K for the slower 0.03-ML/min film deposition rate. A microscopic model of the growth at the $S_B(b)$ and $S_B(n)$ edges is suggested in which we propose that at the $S_B(b)$ edges the accommodation is preferable at existing kink sites whereas at the $S_B(n)$ edges new kinks may be nucleated. The overall growth at the edges will, therefore, preserve the roughness of the edges during the growth. We note that the microscopic model and the computed edge growth coefficient are in qualitative agreement with recent experimental observations of growth using STM microscopy.[1,2] A quantitative comparison between such theoretical simulations and the experimental observations can be made if the adatom-adatom and adatom-surface defect interaction are also incorporated in the dynamics and the simulations are performed on an S_B terrace with varying widths.

Finally, we note that through this work we have not only identified important dynamical processes that may occur during the growth on a single-stepped Si{001} surface but also have set up a frame work of time-dependent kinetic simulations which can be used to compute macroscopic quantities of direct experimental interest.

ACKNOWLEDGMENTS

We gratefully thank the Office of Naval Research and the National Science Foundation for financial support. The Pennsylvania State University supplied a generous grant of computer time for this work.

[1]A. J. Hoeven, J. M. Lenssinck, D. Dijkkamp, E. J. van Loenen, and J. Dieleman, Phys. Rev. Lett. **63**, 1830 (1989).

[2]M. G. Lagally, Y.-W. Mo, R. Kariotis, B. S. Swartzentruber, and M. B. Webb, *Kinetics of Ordering and Growth at Surfaces* (Plenum, New York, 1990), and references therein.

[3]See, for example, M. Tsuchiya, P. M. Petroff, and L. L. Coldren, Appl. Phys. Lett. **54**, 1690 (1989), and references therein.

[4]R. J. Hamers, R. M. Tromp, and J. E. Demuth, Phys. Rev. B **34**, 5343 (1986).

[5]D. E. Aspnes and J. Ihm, Phys. Rev. Lett. **57**, 3054 (1986).

[6]P. E. Wierenga, J. A. Kubby, and J. E. Griffith, Phys. Rev. Lett. **59**, 2169 (1987).

[7]D. J. Chadi, Phys. Rev. Lett. **43**, 43 (1987).

[8]S. J. Pennycook and D. E. Jesson, Phys. Rev. Lett. **64**, 938 (1990).

[9]D. E. Jesson, S. J. Pennycook, and J.-M. Baribeau, in *High Resolution Electron Microscopy of Defects in Materials,* edited by R. Sinclair, D. J. Smith, and U. Dahmen, MRS Symposium Proceedings No. 183 (Materials Research Society, Pittsburgh, 1990), p. 223.

[10]D. E. Jesson, S. J. Pennycook, and J.-M. Baribeau, Phys. Rev. Lett. **66**, 750 (1991).

[11]T. W. Poon, S. Yip, P. S. Ho, and F. F. Abraham, Phys. Rev. Lett. **65**, 2161 (1990).

[12]E. Pehlke and J. Tersoff, Phys. Rev. Lett. **67**, 465 (1991).

[13]O. L. Alerhand, D. Vanderbilt, R. D. Mead, and J. D. Joannopoulos, Phys. Rev. Lett. **61**, 1973 (1988).

[14]D. Vanderbilt, O. L. Alerhand, R. D. Mead, and J. D. Joannapoulos, J. Vac. Sci. Technol. B **7**, 1013 (1989).

[15]O. L. Alerhand, A. N. Berker, J. D. Joannapoulos, D. Vanderbilt, R. J. Hamers, and J. E. Demuth, Phys. Rev. Lett. **64**, 2406 (1990).

[16]E. Pehlke and J. Tersoff, Phys. Rev. Lett. **67**, 1290 (1991).

[17](a) C. Roland and G. H. Gilmer, Phys. Rev. Lett. **67**, 3188 (1991); (b) Z. Zhang, Y. T. Lu, and H. Metiu, Phys. Rev. B **46**, 1917 (1992).

[18]F. Stillinger and T. Weber, Phys. Rev. B **31**, 5262 (1985).

[19]J. Tersoff, Phys. Rev. B **39**, 5566 (1989).

[20]A. F. Voter and J. D. Doll, J. Chem. Phys. **82**, 80 (1985); A. F. Voter, Phys. Rev. A **34**, 6819 (1986).

[21]D. Srivastava and B. J. Garrison, J. Chem. Phys. **95**, 6885 (1991).

[22]D. Srivastava and B. J. Garrison, Phys. Rev. B **46**, 1472 (1992).

[23]I. P. Batra, Phys. Rev. B **41**, 5048 (1990).

[24]F. F. Abraham, Adv. Phys. **35**, 1 (1986).

[25]H. J. C. Berendsen, J. P. M. Postma, W. F. van Gunsteren, A. Dinola, and J. R. Haak, J. Chem. Phys. **81**, 3684 (1984).

[26]D. Srivastava, B. J. Garrison, and D. W. Brenner, Phys. Rev. Lett. **63**, 302 (1989); Langmuir **7**, 683 (1990).

[27]G. Brocks, P. J. Kelly, and R. Car, Phys. Rev. Lett. **66**, 1729 (1991).

[28]Z. Zhang, Y. T. Lu, and H. Metiu, Surf. Sci. **50**, L248 (1991).

[29]C. P. Toh and C. K. Ong, Phys. Rev. B **45**, 11 120 (1992).

[30]Y.-W. Mo, J. Kleiner, M. B. Webb, and M. G. Lagally, Phys. Rev. Lett. **66**, 1998 (1991); Y.-W. Mo, R. Kariotis, B. S. Swartzentruber, M. B. Webb, and M. G. Lagally, J. Vac. Sci. Technol. A **8**, 201 (1990).

[31]R. J. Hamers, U. K. Kohler, and J. E. Demuth, Ultramicroscopy **31**, 10 (1989).

[32]M. G. Lagally, R. Kariotis, and Y.-W. Mo, Ultramicroscopy **31**, 87 (1989).

[33]J. Y. Tsao, E. Chason, U. Köhler, and R. Hamers, Phys. Rev. B **40**, 11 951 (1989).